

**FIRST EVER CIRCULAR POLARIZATION RATIO (CPR) AND RADAR SCATTERING MAP OF LUNAR POLES IN L-BAND USING FULL-POL CHANDRAYAAN-2 DFSAR DATA.** Tarun Maganti\*, Tathagata Chakraborty, Deepak Putrevu, Sriram S. Bhiravarasu, Anup Das, Dharmendra Kr. Pandey, V.M.Ramanujam, Raghav Mehra and Shubham Gupta, Space Applications Center, ISRO, Ahmedabad, India. \*([tarunm@sac.isro.gov.in](mailto:tarunm@sac.isro.gov.in))

**Introduction:** Dual-Frequency Synthetic Aperture Radar (DFSAR) onboard Chandrayaan-2 orbiter is state-of-the-art SAR sensor for planetary mission. The architecture of this radar instrument is capable to acquire data in L- & S-bands in both full and hybrid-polarimetric modes, with varying resolution maximum up to 2m/pixel<sup>[1]</sup>. Consequently, DFSAR observations can make a substantial contribution to the mapping and characterisation of several geomorphological features on the moon<sup>[2-4]</sup>. Presently, a lot of fully polarimetric operational mode is producing a lot of data. Our in-house developed software Microwave Data Analysis Software (MIDAS) is freely available to users (<https://vedas.sac.gov.in/static/soft/Midas-windows.zip>) for DFSAR data processing. To minimize the extensive efforts for analysing individual dataset, mosaics of frequently utilised polarimetric products have been generated. Further, the mosaics will be beneficial for regional studies of the lunar surface features.

**Methodology:** The automation code was written in Python 3, but the polarimetric data processing was done using MIDAS<sup>[5]</sup> binaries. Each dataset has been multilooked using the following formula:

$$\text{Multilook Factor} = \frac{\text{Line Spacing}}{\text{Pixel Spacing} \times \sin(\theta)}$$

Around 300 datasets acquired upto season 3 are processed to generate the mosaics. The used process is depicted by the flow chart in *Figure 1*.

The following products were generated.

1) *Circular Polarization Ratio:* Circular Polarization Ratio (CPR)<sup>[6-7]</sup> is an important function in characterization of craters and other lunar surfaces<sup>[2-4]</sup>. Stokes parameters computed

from Sinclair Matrix are used to generate CPR<sup>[5]</sup>.

2) *Polarimetric Decompositions:* Polarimetric decompositions are incredibly valuable for understanding the scattering mechanisms of a target.

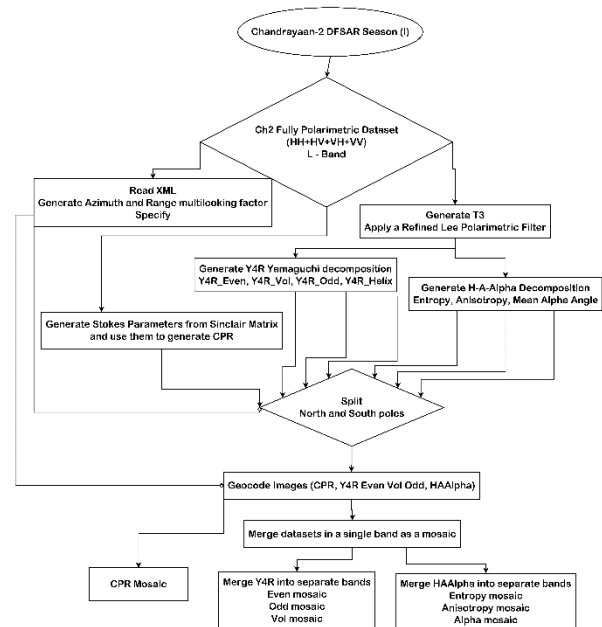


Figure 1: Flow chart of the process

a) *Yamaguchi four component decomposition (orientation angle corrected):* Y4R decomposes the target based upon Bragg's scattering mechanism as Single bounce component, Randomly oriented dipoles as Volumetric component, Dihedral corner reflector mechanism as Double bounce component and non-uniformly oriented dipoles mechanism by a Helix component. Y4R has an orientation angle correction over the original Yamaguchi four component and is preferred<sup>[8-9]</sup>.

b) *H-A-Alpha Decomposition:* Entropy (H), Anisotropy (A), and Mean Alpha Angle ( $\bar{\alpha}$ )<sup>[10]</sup> are eigenvalue based polarimetric

decompositions that do not presume an underlying statistical distribution and are not restricted by physical constraints imposed by the models. Entropy ( $H$ ) represents the degree of disorder in the scatterer and the depolarization of the microwave energy.  $H < 0.3$  indicates that scatterers are coherent and highly polarised [11]. High entropy can be produced by distributed targets. Anisotropy is a measure of the relative importance of the second and third eigenvalues and is typically utilised as a distinguishing parameter in situations when  $H > 0.7$ . The mean alpha angle ( $\bar{\alpha}$ ) characterises both the nature of the scatterer and the type of scattering induced by the target.  $\bar{\alpha} \in [0, 40^\circ]$  indicates surface scattering,  $\bar{\alpha} \in [40^\circ, 60^\circ]$  indicates volume scattering, and  $\bar{\alpha} \in [60^\circ, 90^\circ]$  indicates double bounce scattering from the target [10].

- 3) *Geocoding and Ortho-rectification*: DFSAR data products are georeferenced and orthorectified using LOLA DEM with 120m/pix spatial resolution, to obtain SAR derived polarimetric products of 25m pixel spacing in both azimuth and range direction.

- 4) *Mosaics*: The resultant polarimetric products have been divided into North and South poles and respective mosaics were generated using GDAL. Gdal merge function was updated to average the values in the overlapping parts instead of default overwriting. Currently datasets obtained in the initial three SAR data acquisition seasons (Sept 2019 – Nov 2020) are mosaicked (Fig. 2). The season 4 to season 7 datasets (Dec 2020 – Till Date) are under process. The mosaics will be published on ISRO's Pradan website (<https://pradan.iisd.gov.in/ch2>).

*References*: [1] Putrevu, D. et al. (2016) Adv. Space Res., 57, 627- 646. [2] Putrevu, D. et al., (2020), 51<sup>st</sup> LPSC, Abstract#1420. [3] Chakraborty, T. et al., (2021), 52<sup>nd</sup> LPSC, Abstract#1447. [4] Bhiravarasu, et al., (2021), PSJ, 2, 134, DOI: 10.3847/PSJ/abdfbf. [5] Tarun, M. et al., (2022), 53<sup>rd</sup> LPSC, Abstract#2232 [6] Raney, R.K. et al. (2012) JGR, 117, E00H21. [7] Raney, R. K. et al., (2011), in Proceedings of the IEEE, 99, 5, 808-823. [8] Lee, J.S., and Ainsworth, T.L. (2010) IEEE TGRS, 49(1), 53-64. [9] Yamaguchi, Y. et al. (2010) IEEE TGRS, 49(6), 2251-2258. [10] Cloude, S.R., and Pottier, E. (1997) IEEE TGRS, 35(1), 68-78. [11] Singh, G. et al. (2013) IEEE TGRS, 52(2), 1177-1196.

## Results:

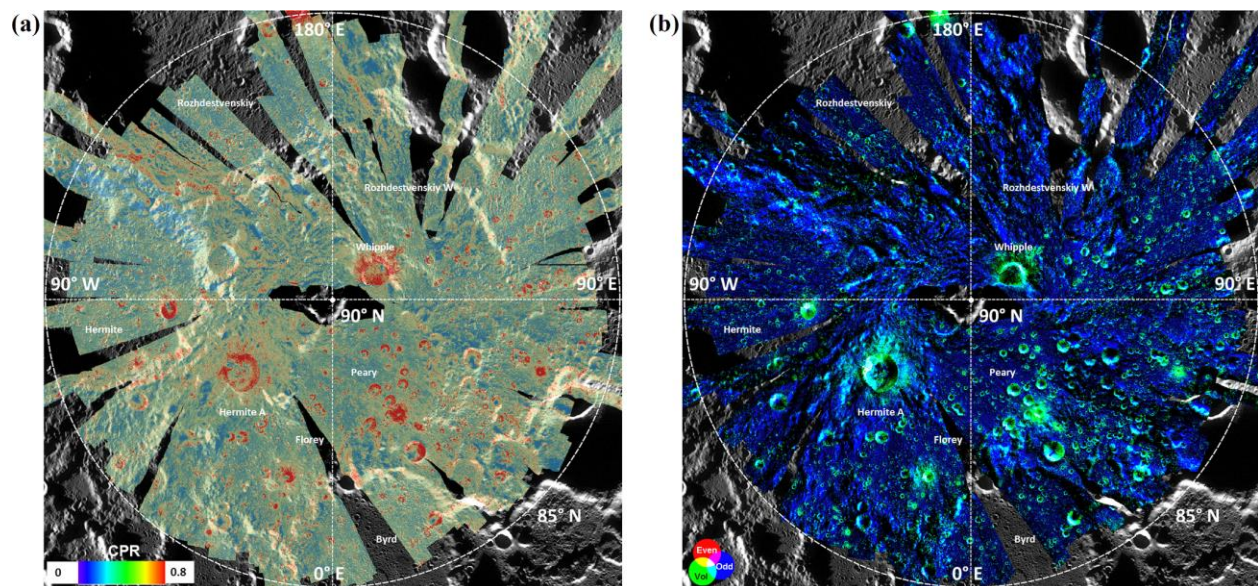


Fig. 2: (a) CPR map of North pole (85°N to 90°N), (b) Yamaguchi decomposition (Y4R) map of North pole derived from L-band Full-pol DFSAR data.